Iranian Society of Acoustics and Vibration
The 13th ISAV2023 International Conference on Acoustics and Vibration
20, 21 Dec 2023 Tehran - Iran

The influencing parameters on the sound insulation performance of membrane-type acoustic metamaterials with central local resonator

Erfan Asgari[a], Abdolreza Ohadi[b*], Reza Hedayati[c]

[a] *M.Sc. student, Acoustics Research Lab., Department of Mechanical Engineering, Amirkabir University of Technology (Tehran Polytechnic), Tehran, Iran.*

[b] *Professor, Acoustics Research Lab., Department of Mechanical Engineering, Amirkabir University of Technology (Tehran Polytechnic), Tehran, Iran.*

[c] *PhD, Department of Mechanical Engineering, Amirkabir University of Technology (Tehran Polytechnic), Tehran, Iran.*

** Corresponding author e-mail: a_r_ohadi@aut.ac.ir*

Abstract

Membrane-type Acoustic Metamaterials (MAMs) effectively control low-frequency sound, surpassing conventional materials with excellent insulation capabilities. Remarkably, acoustic metamaterials with negative dynamic mass density exhibit a significant increase in sound transmission loss (STL) within a narrow frequency range. In general, the performance of material insulation involves examining factors such as dip and peak frequencies, and bandwidths of STL curves. Moreover these factors can be precisely tuned by adjusting membrane and resonator physical properties, demonstrating the adaptability of MAMs. In this study, employing parametric analysis using COMSOL Multiphysics software with impedance tube testing method, the impact of parameters such as local resonator (disk) mass, resonator radius, membrane pre-tension, and membrane thickness on the performance of sound insulation by these metamaterials was investigated. Sensitivity analysis was employed to assess the impact of various parameters on the metamaterial's insulation performance. The sensitivity analysis results indicate that the first dip frequency is most sensitive to the resonator mass, decreasing by 19.5% from its initial value with an increase in resonator mass. The second dip frequency, peak frequency, and bandwidth are most sensitive to the resonator radius, increasing by 26.5%, 58.3%, and 74.7% of their initial values, respectively, with an increase in radius. It is worth noting that membrane thickness has no effect on the first dip frequency, peak frequency, and bandwidth. Therefore, considering various needs in industries, residential buildings, etc., for sound insulation purposes, optimizing insulation within a desired frequency range can be achieved by adjusting the noted influential parameters of metamaterials according to specific requirements.

Keywords: Membrane-type Acoustic Metamaterials; Sound transmission loss; Insulation performance; Sensitivity analysis.

1. Introduction

Effective noise control, especially concerning low-frequency noise, holds immense importance in the aerospace, ground transportation, and ship design and production sectors [1]. Low-frequency noise, characterized by its lengthy wavelength, poses challenges in insulation due to its strong penetrating power and slow attenuation during propagation. Adding to the complexity, human organs predominantly resonate at low frequencies, making this type of noise more detrimental to both physical and mental health. Traditional acoustic materials, following the mass law of sound insulation, require substantial thickness to insulate low-frequency noise, conflicting with the demand for lightweight equipment [2]. Acoustic metamaterials do not adhere to the mass law and due to their unique acoustic properties, exhibit significantly higher sound transmission loss compared to predictions based on the mass law. Therefore, the development of new lightweight materials or structures is essential for effective low-frequency noise control. Therefore, the design of new lightweight materials or structures to achieve low-frequency noise control is of utmost importance.

Yang et al. [3] introduced a high-density core at the elastic membrane's centre to modify its vibration mode, leading to a negative effective density at 200–300 Hz and enabling total reflection of low-frequency sounds. This innovative structure not only meets the requirements for low-frequency noise reduction but also holds potential for lightweight design. Consequently, researchers have proposed diverse structural design strategies to enhance the low-frequency sound insulation capabilities of membrane-type acoustic metamaterials (MAMs). To achieve similar low-frequency sound insulation peaks, Membrane-Type Acoustic Metamaterials (MAMs) can significantly reduce weight compared to homogeneous plates, as dictated by the mass law, offering a notable lightweight advantage. In a study by Naify et al. [4] a structure was engineered using a circular polyetherimide membrane with an attached mass, bonded to a rigid support frame with epoxy resin. By adjusting the thermoforming temperature of the epoxy resin to control tension, they created a structure with a 500% increase in maximum sound insulation compared to mass law predictions. Furthermore, through parametric and structural dynamics analysis, they determined that tuning the number, radius, and distribution of the mass block in a membrane-type locally resonant acoustic metamaterial with an annular mass block resulted in a 360% expansion of the sound insulation bandwidth above 30 dB compared to a cylindrical mass block of equal weight [5-6].

In this study, we use the sensitivity analysis method to assess the level of effect of different geometrical and physical parameters on the sound insulation performance. Sensitivity analysis is a method that quantitatively evaluates the effect of different parameters on the performance of a system, which makes it easier to make decisions about the selection of design parameters. The parameters considered in this study include local resonator mass, resonator radius, membrane pre-tension and thickness. Also, sound insulation performance factors include peak frequency and bandwidth. The aim of this research is to reach to quantitative conclusions about the relationship between dimensional and physical characteristics and optimal performance of sound insulation in membrane-type metamaterials.

2. Materials and methods

2.1 Design and geometry

The impedance tube testing method involves employing a tube with a sound source attached at one end and placing the test sample inside. To evaluate transmission loss, four microphones are strategically positioned on each side of the sample, their diaphragms flush with the tube's inner surface [7]. Plane waves are generated within the tube using a wide noise signal. The resultant standing wave pattern is analysed by measuring sound pressure at the four locations and scrutinizing their relative amplitude and phase. The acoustic transfer matrix is computed based on the pressure and particle velocity (or acoustic impedance) of the traveling waves on either side of the material. This matrix enables the extraction of transmission loss and several other critical acoustic properties, including the

normal incidence sound absorption coefficient. This comprehensive approach provides a detailed understanding of the material's acoustic behaviour, essential for various applications requiring precise sound control and insulation. The termination of the tube is arbitrary in principle, but experience has found that the most useful termination is at least weakly anechoic, causing minimal reflection of the sound wave back down the tube, as illustrated in Figure 1.

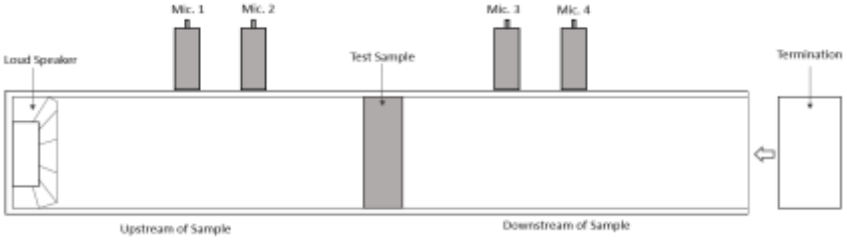

Figure 1. Schematic representation of 4-mic wave impedance tube

In accordance with Figure 2, the metamaterial studied in this research comprises a disk-shaped resonator coupled with a circular membrane. The resonator undergoes localized vibrations on the membrane. The response of the system, such as the dip frequencies and a peak frequency, as well as the bandwidth of the metamaterial, is expected to be influenced by four parameters: the resonator mass, the radius of the disk, the pre-tension of the membrane, and the thickness of the membrane.

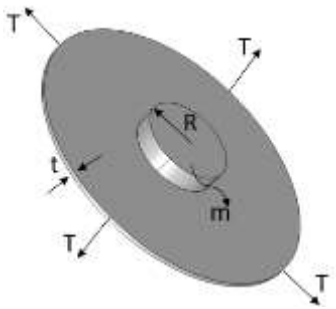

Figure 2. Schematic of membrane-type metamaterial with investigated parameters. m: Resonator mass - R: Resonator radius - T: Membrane pre-tension - t: Membrane thickness

Table 1. Material properties and parameters of membrane and mass

	Membrane	Local resonator
Mass density (kg/m3)	980	7800
Young's modulus (Pa)	2×10^5	2×10^{11}
Poisson's ratio	0.49	0.33
Thickness (mm)	0.32	-
Total mass (mg)	-	400
Radius (mm)	10	4
Pretension (N/m)	75	-

2.2 FEM simulation

In this study, COMSOL Multiphysics package is utilized to model impedance tube with a membrane-type metamaterial at its centre to calculate sound transmission losses. The membrane component is simulated utilizing membrane physics, the disk segment is designed using solid mechanics physics, and the acoustic section is simulated using pressure acoustic-frequency domain physics. Given the presence of the three distinct noted physics, three distinct physical interactions are required for this problem. The first interaction occurs between the disk and the membrane, the second involves acoustic waves and the membrane, and the third pertains to acoustic waves and the disk. By utilizing the model presented in Section 2.1 and considering the parameters outlined in Table 1 as a basis, the

study explores the impact of both geometrical and material properties of the membrane and local resonator on the sound insulation peak frequency and the bandwidth of the Membrane-type Acoustic Metamaterials (MAMs).

3. Results

3.1 Validation

In this section, first, the accuracy of the results presented by Sabet et al. [8] in calculating the sound transmission loss of a sample disk made of polycarbonate material is validated, aiming to achieve optimal acoustic boundary conditions for precise modelling of impedance tube and accurate mechanical boundary conditions for the sample. Subsequently, the validation of the results obtained by Yang et al. [9] in calculating the sound transmission loss of a metamaterial with a central local resonator is addressed, serving the same purpose. Figure 3(a) illustrates the comparison between the results obtained by Sabet et al. and the simulations conducted in our study. As evident, the system consistently follows a similar trend in all cases, and the dip frequencies are almost located within the same range. Their numerical work involved writing custom code and did not utilize any specific finite element software. In their numerical study, the dip frequency was reported as 540 Hz with a sound transmission loss of 15 dB, while in their experimental work, these values were 530 Hz and 5 dB, respectively. In the simulations performed for the polycarbonate sample using COMSOL Multiphysics in our study, the dip frequency is calculated as 571 Hz with a corresponding sound transmission loss of 9 dB. In Figure 3(b), the validation of our study results with the findings of Yang et al. is presented. It is evident that the system's behaviour exhibits a similar pattern in both studies. The two dip frequencies and the peak frequency in both studies almost overlap and are equal to 145 Hz, 970 Hz, and 265 Hz, respectively.

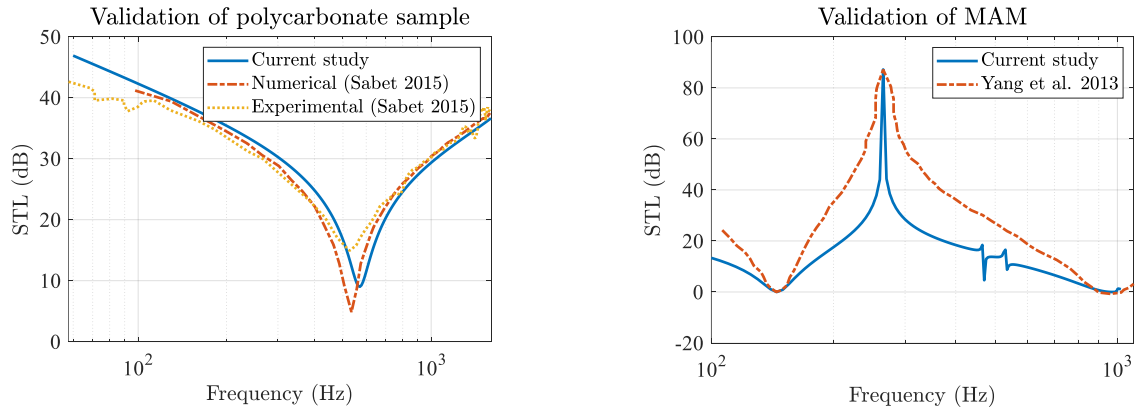

Figure 3. (a) Validation of polycarbonate sample. (b) Validation of MAM.

3.2 Parametric study

The sound insulation performance of membrane-type metamaterials is generally determined by three key factors: locations of dip frequencies, location of peak frequency, and effective bandwidth (frequency bandwidth with sound transmission loss above 20 dB). In this section, we focus on investigating these three factors influence on the metamaterial's performance in sound insulation. All the metamaterial specifications previously mentioned in Table 1 remain constant, with only one of the parameters such as local resonator mass, resonator radius, membrane pre-tension, and membrane thickness being altered. Figures 4(a), 5(a), 6(a), and 7(a) and Figures 4(b), 5(b), 6(b), and 7(b) illustrate the transmission loss variations as a function of frequency and the influence of influential factors on the sound insulation performance in terms of frequency for each of these cases, respectively. Each of these parameters is varied in four equal steps, and the results are compared.

As shown in Figure 4(b), when the mass of the local resonator is increased, both the first dip frequency and peak frequency are reduced and both the second dip frequency and bandwidth remain almost unchanged. When the mass of the local resonator is increased from 250 mg to 400 mg, the first dip frequency is reduced from 215 Hz to 173 Hz, the peak frequency is reduced from 475 Hz to 380 Hz, the second dip frequency is almost unchanged, and its value is approximately 1290 Hz, and the bandwidth is almost unchanged and its value is approximately 342 Hz.

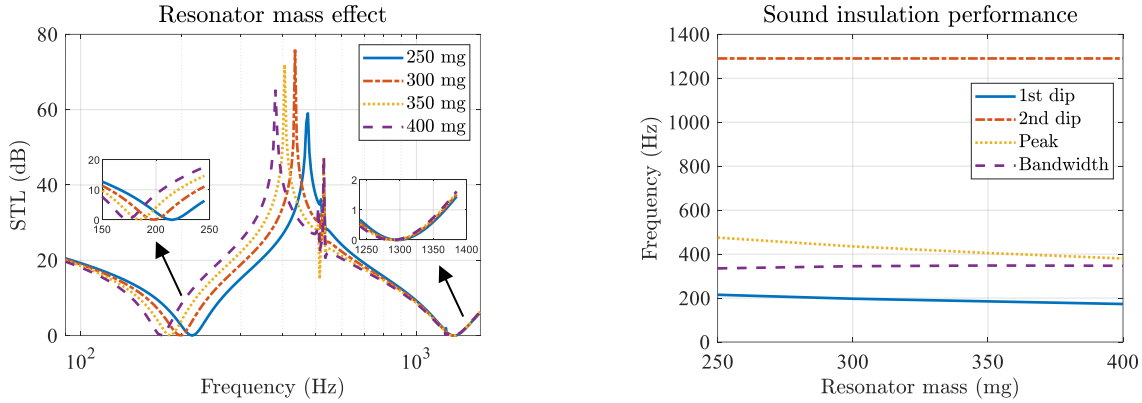

(a) (b)

Figure 4. (a) Effect of resonator mass on STL-frequency curves. (b) Influence of resonator mass on sound insulation performance of MAMs.

As shown in Figure 5(b), when the radius of the local resonator is increased, the first dip frequency remains almost unchanged, while the peak frequency, second dip frequency, and bandwidth increase. When the radius of the local resonator is increased from 2.5 mm to 4 mm, the first dip frequency is changes slightly from 142.5 Hz to 173 Hz, the peak frequency increases from 240 Hz to 380 Hz, the second dip frequency increases from 1020 Hz to 1290 Hz, and the bandwidth increases from 199 Hz to 347 Hz.

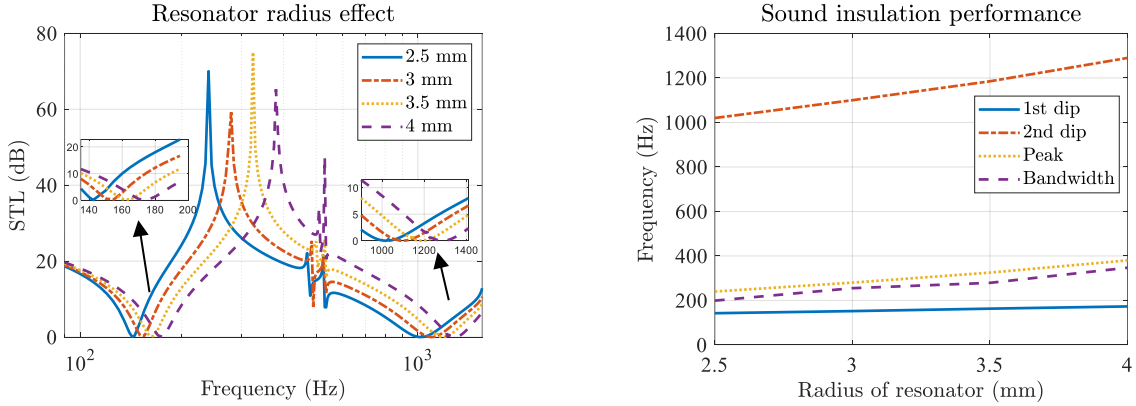

(a) (b)

Figure 5. (a) Effect of resonator radius on STL-frequency curves. (b) Influence of resonator radius on sound insulation performance of MAMs.

As shown in Figure 6(b), when the pre-tension of the membrane is increased, the first dip frequency is not sensitive to the change of the pre-tension in the membrane, but the second dip frequency does increase a lot. when the pre-tension of the membrane is increased from 60 N/m to 75 N/m, the first dip frequency is almost unchanged from 155 Hz to 173 Hz, the peak frequency is increased from 240 Hz to 380 Hz, the second dip frequency is significantly increased from 1150 Hz to 1290 Hz and the bandwidth is increased from 285 Hz to 347 Hz.

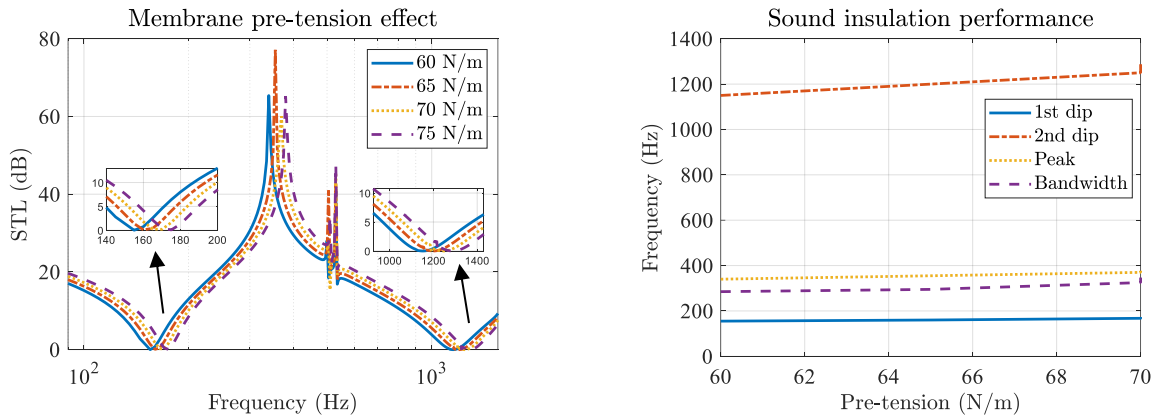

Figure 6. (a) Effect of membrane pre-tension on STL-frequency curves. (b) Influence of membrane pre-tension on sound insulation performance of MAMs.

As shown in figure 7(b), when the thickness of the membrane is increased, the first dip frequency, the peak frequency and the bandwidth are not sensitive to the change of the pre-tension in the membrane. The increase of the thickness of the membrane can only reduce the second dip frequency. When the thickness of the membrane is increased from 0.26 mm to 0.32 mm, the first dip frequency, the peak frequency and the bandwidth are 173 Hz, 380 Hz and 347 Hz, respectively. The second dip frequency is decreased from 1425 Hz to 1290 Hz.

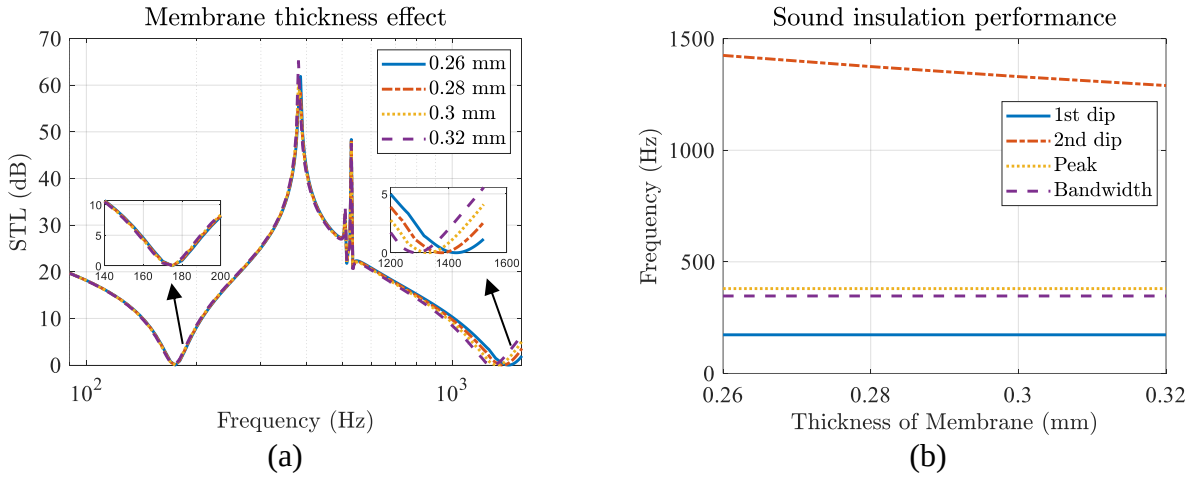

Figure 7. (a) Effect of membrane thickness on STL-frequency curves. (b) Influence of membrane thickness on sound insulation performance of MAMs.

4. Discussion

4.1 Investigating the performance of metamaterial insulation based on vibration modes

The acoustic behavior of the MAM deviates from predictions made by the conventional mass density law. Two distinct dips in transmission loss are observed in the MAM's two lowest piston-like motions, separated by a peak frequency. Analysis of the mode shapes depicted in Figure 8 reveals that the first dip is a result of the eigenmode where the membrane and attached mass vibrate in phase, while the second dip is solely due to the membrane's motion. The frequency positions of the two sound insulation dips correspond to the first and second piston-like motion eigenmodes of the metamaterial.

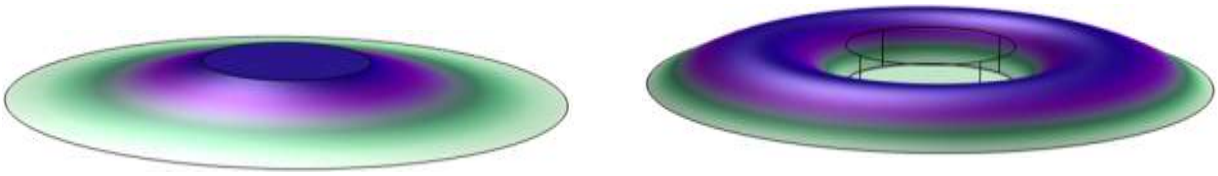

(a) (b)

Figure 8. (a) First piston-like motion eigenmode. (b) Second piston-like motion eigenmode.

To interpret the physical mechanism of MAM, its dynamic effective mass density, defined as $\rho_{eff} = \frac{\langle p_1 - p_2 \rangle}{\langle a_z \rangle}$, plays a key role, where p_1 and p_2 denote the incident sound pressure and transmitted sound pressure, respectively, and $\langle a_z \rangle$ represents the average acceleration of metamaterial in the incident direction. Starting from the frequency of the first dip, the effective mass density transitions from positive to negative values, reaching negative infinity around the peak frequency. It then abruptly shifts to positive infinity and gradually decreases to zero at the frequency of the second dip. This behavior can also be explained by the displacement field of the membrane $\langle W \rangle$, where W is associated with a piston-like motion of the MAM. Yang et al. [9] demonstrated a strong correlation between the transmitted sound intensity and the average displacement along the sound propagation axis. At the peak frequency $\langle W \rangle = 0$, ρ_{eff} approaches infinity according to the definition of effective mass density. The relationship between sound speed and effective mass density is represented by $c = \sqrt{\frac{\beta_{eff}}{\rho_{eff}}}$, where β_{eff} denotes the effective bulk modulus. At the peak frequency, where the effective mass density becomes infinite, the sound speed becomes zero, resulting in the absence of sound propagation. In frequency ranges where the effective mass density becomes negative, the sound speed transforms into a pure imaginary number, causing sound propagation to exponentially decay and transform into an evanescent wave. These characteristic frequencies (such as peak and dip frequencies) are determined by the resonant and anti-resonant coupling characteristics of the structural and the sound field. For the anti-resonant mode of the system, the vibration of the local resonator is out-of-phase with the membrane, therefore, the sound transmission loss peak appears in the sound transmission loss profile.

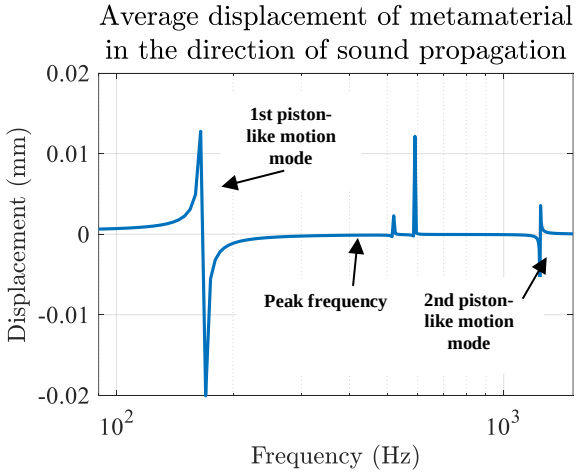

Figure 9. Average displacement of metamaterial in the direction of sound propagation versus frequency.

Figure 9 illustrates the average displacement of the metamaterial along the direction of sound propagation versus frequency. As mentioned earlier, sound transmission correlates with the average displacement of the membrane and resonator directly. At the first and second dip frequencies, the highest average displacements of the membrane and resonator along the direction of sound propagation exist. Consequently, sound transmission loss is minimal at these frequencies. In Figure 9, the

peak frequency location of the STL diagram is indicated. The average displacements of the membrane and resonator are nearly zero at the peak frequency. This implies that sound transmission through the metamaterial is at its minimum.

4.2 Investigating the change of parameters on the performance of metamaterial insulation

As mentioned earlier, the vibrational behavior of the metamaterial around its dip frequencies is very close to that of piston-like motion modes According to Figure 8a, the vibration behavior of the system around the first dip frequency can be modeled as a simple spring-mass system, where its natural frequency is given by $\sqrt{\frac{k}{m}}$. Here, k represents the system's stiffness, directly related to the pre-tension of the membrane, and m is the mass of the resonator. Consequently, it is expected that with an increase in membrane pre-tension and resonator mass, the value of the first dip frequency will increase and decrease, respectively. In this mode, the vibrational behavior of the system is mainly influenced by the motion of the resonator; thus, the first dip frequency undergoes significant changes concerning the resonator mass. Moreover, by increasing the resonator's radius, since the common area between the resonator and the membrane increases, the system's stiffness also increases. Therefore, an increase in the resonator's radius can lead to an increase in the first dip frequency. The results in Figures 4 to 7 confirm the validity of the stated observations.

In the second dip frequency mode, contrary to the first dip frequency, the metamaterial's vibrational behavior closely resembles the second piston-like mode. In this vibration mode, the system's motion is strongly influenced by the membrane oscillations, where the membrane's natural frequency significantly dominates the system's natural frequency. As shown in Figure 8b, the resonator remains stationary in this vibrational mode, and only the membrane undergoes vibrations. The membrane's natural frequency is proportional to the mathematical equation $\sqrt{\frac{T}{\rho t a^2}}$, where T represents the membrane pre-tension, ρ is the membrane's mass density, t is the membrane thickness, and a is the effective radius of the membrane. Therefore, the membrane's natural frequency has a direct relationship with its pre-tension and an inverse relationship with its thickness and effective radius. Consequently, increasing the membrane pre-tension and thickness results in an increase and decrease in the second dip frequency, respectively. By increasing the resonator's radius, the effective radius of the membrane decreases. Considering that the membrane's natural frequency has an inverse relationship with its effective radius, increasing the resonator's radius leads to an increase in the second dip frequency. As the resonator remains stationary in this vibrational mode, any change in its mass does not affect the second dip frequency. The results in Figures 4 to 7 confirm the statements about the second dip frequency. The peak frequency of the system generally follows the trends of both the first and second dip frequencies. For example, the first dip frequency has the most significant impact concerning changes in the resonator's mass, while the second dip frequency remains unaffected by changes in the resonator's mass. Since the peak frequency is directly related to both the first and second dip frequencies, it is expected that the peak frequency decreases with an increase in the mass. Figure 4 accurately demonstrates the statements about the peak frequency.

4.3 Sensitivity analysis

To assess the impact of various parameters on the dip and peak frequencies and bandwidth of STL curves, the sensitivity of sound insulation dip and peak frequencies and bandwidth to these different parameters is defined as follows:

$$S_i = \frac{|f_{i2} - f_{i1}|}{x_{i2}/x_{i1}} \tag{1}$$

Where x_i represents the i^{th} design parameter, f_i corresponds to the i^{th} dip/peak or bandwidth frequency associated with the i^{th} design parameter. Subscript 1 denotes the minimum value of the design parameter, while subscript 2 indicates its maximum value.

Table 2. Sensitivity of sound insulation first dip frequency to different parameters.

Parameters	Local resonator mass	Disk radius	Membrane pre-tension	Membrane thickness
Sensitivity	26.25	19.06	15.43	0

Table 3. Sensitivity of sound insulation second dip frequency to different parameters.

Parameters	Local resonator mass	Disk radius	Membrane pre-tension	Membrane thickness
Sensitivity	0	168.75	120	109.69

Table 4. Sensitivity of sound insulation peak frequency to different parameters.

Parameters	Local resonator mass	Disk radius	Membrane pre-tension	Membrane thickness
Sensitivity	59.375	87.5	34.28	0

Table 5. Sensitivity of sound insulation bandwidth to different parameters.

Parameters	Local resonator mass	Disk radius	Membrane pre-tension	Membrane thickness
Sensitivity	8.125	92.5	53.14	0

Table 2 illustrates the sensitivity analysis results for the first dip frequency. As mentioned earlier, the oscillatory behavior of the system around this frequency can be modeled as the simple vibrations of a mass-spring system. The natural frequency of the system is significantly influenced by the mass of the oscillating resonator. The sensitivity analysis results effectively validate this statement. As shown in Table 2, the first dip frequency exhibits the highest sensitivity, in descending order, to the resonator mass, disk radius, and membrane pre-tension. This frequency shows no sensitivity to changes in the membrane thickness.

Table 3 presents the sensitivity analysis results for the second dip frequency. As previously mentioned, the system's oscillatory behavior around this frequency is highly dependent on membrane vibrations since the resonator remains motionless in this mode of vibration. As stated in section 4.2, the system's natural frequency is derived from the natural frequency of the membrane. This frequency has a direct relationship with the square root of membrane pre-tension and an inverse relationship with the square root of membrane thickness. The second dip frequency has an inverse relationship with the effective radius of the membrane. Considering that the effective radius and not its square root is inversely related to the natural frequency, it is expected that this frequency exhibits the highest sensitivity to the resonator's radius. Table 3 effectively proves this statement. In descending order, this frequency shows the highest sensitivity to the resonator radius, membrane pre-tension, and membrane thickness. Since the resonator remains motionless at this frequency, it does not exhibit any sensitivity to the resonator mass.

Table 4 displays the sensitivity analysis results for the peak frequency. As mentioned in section 4.2, the peak frequency is a function of the behaviors of the first and second dip frequencies. Since the resonator mass and effective membrane radius have the most significant impact on these two frequencies, it is expected that the peak frequency exhibits the highest sensitivity to these parameters.

Table 4 effectively confirms this statement. In descending order, the peak frequency shows the highest sensitivity to the resonator radius, resonator mass, and membrane pre-tension. This frequency does not exhibit any sensitivity to membrane thickness.

Table 5 presents the sensitivity analysis results for the bandwidth. Bandwidth exhibits the highest sensitivity, in descending order, to the resonator radius, membrane pre-tension, and resonator mass. It does not show any sensitivity to membrane thickness.

5. Conclusions

In this paper, the influence of mass of local resonator, disk radius, membrane pre-tension, and membrane thickness on the performance of membrane-type metamaterial insulation was studied. The factors representing the performance of this metamaterial insulation include the locations of dip frequencies, peak frequency, and bandwidth of the sound transmission loss curves. Sensitivity analysis was employed to assess the impact of various parameters on the metamaterial's insulation performance. The sensitivity analysis results indicate that the first dip frequency is most sensitive to the resonator mass, decreasing by 19.5% from its initial value as a result of an increase in resonator mass. The second dip frequency, peak frequency, and bandwidth are most sensitive to the resonator radius, increasing by 26.5%, 58.3%, and 74.7% of their initial values, respectively, as a result of an increase in radius. It is worth noting that membrane thickness has no effect on the first dip frequency, peak frequency, and bandwidth. Considering that increasing the resonator radius enhances system stiffness, it can be concluded that this parameter is the most influential design parameter in determining the insulation performance factors of the metamaterial.

REFERENCES

1. V. Mallardo, M.H. Aliabadi, A. Brancati, et al., “An accelerated BEM for simulation of noise control in the aircraft cabin”, *Aerospace Science and Technology* **23**(1) 418–428 (2012).
2. T.D. Rossing, Springer Handbook of Acoustics, Springer Science+Business Media, New York, 2007.
3. Z. Yang, J. Mei, M. Yang, et al., “Membrane-type acoustic metamaterial with negative dynamic mass”, *Physical Review Letters* **101**(20) 204301 (2008).
4. C.J. Naify, C.M. Chang, Mcknight, et al., “Transmission loss and dynamic response of membrane-type locally resonant acoustic metamaterials”, *Journal of Applied Physics* **108**(11) (2010).
5. C.J. Naify, C.M. Chang, G. Mcknight, et al., “Transmission loss of membrane-type acoustic metamaterials with coaxial ring masses”, *Journal of Applied Physics* **110**(12) (2011).
6. C.J. Naify, C.M. Chang, G. Mcknight, et al., “Scaling of membrane-type locally resonant acoustic metamaterial arrays”, *Journal of the Acoustical Society of America* **132**(4), 2784–2792 (2012).
7. ASTM E2611-09, “Standard Test Method for Measurement of Normal Incidence Sound Transmission of Acoustical Materials Based on the Transfer Matrix Method”.
8. Sabet, S.M. and Ohadi, A, “Experimental and theoretical investigation of sound transmission loss for polycarbonate, poly (methyl methacrylate), and glass”. *Journal of Applied Polymer Science* **133**(7), (2016).
9. Chen, Y., Huang, G., Zhou, X., Hu, G. and Sun, C.T., “Analytical coupled vibroacoustic modeling of membrane-type acoustic metamaterials: Membrane model”. *The Journal of the Acoustical Society of America* **136**(3), 969-979 (2014).